

RESONANT CONVERSION OF THE POINT-SOURCE FIELD TO MULTIPOLE RADIATION USING RING LAYER OF THE OVERCRITICAL PLASMA

A. P. Anyutin,¹ I. P. Korshunov,^{2*} and
A. D. Shatrov²

UDC 538.566.2+621.372.8

We study numerically the two-dimensional problem of excitation of a hollow round cylinder, which is made of a nonmagnetic material with $\mu = 1$ and the negative dielectric permittivity $\varepsilon < 0$, by a filamentary source. It is found that when the relative dielectric permittivity is close to -1 , high- Q resonances exist in hollow cylinders having electrically small diameters. We show that when the source of a cylindrical wave is located within the cavity, undirected radiation is converted at the resonance frequency into multipole radiation with a great number of identical lobes in the radiation pattern. The patterns of the near and far fields are calculated. The influence of the loss on the resonance properties is studied.

1. INTRODUCTION

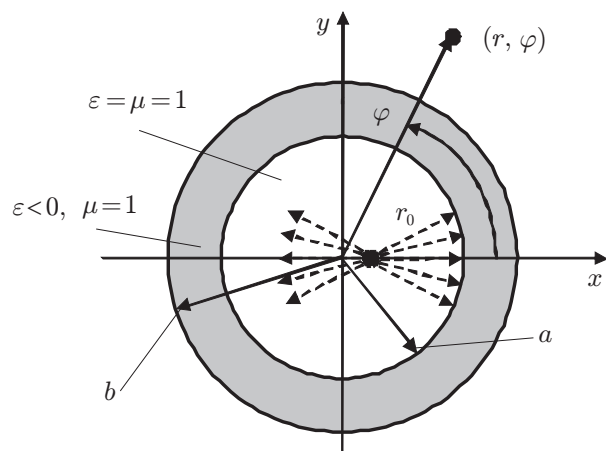


Fig. 1. Geometry of the problem.

In [1], we studied the two-dimensional problem of diffraction of a cylindrical wave by a hollow cylinder of a metamaterial with the dielectric permittivity $\varepsilon < 0$ and the magnetic permeability $\mu < 0$. High- Q resonances, which occur in cylinders with electrically small diameters for dielectric permittivities close to -1 , were discovered and studied for the case of the TM polarization. It was shown that such a structure can be considered as a high- Q ring-shaped resonator cavity with a very slow surface wave of the cylindrical layer.

2. PROBLEM FORMULATION

This paper considers the problem about excitation of a ring-shaped layer of overdense plasma or a metamaterial with $\varepsilon < 0$ and $\mu = 1$ by a filamentary source. The

case of the TM polarization is considered, and it is assumed that the source is located within the ring-shaped layer (see Fig. 1).

The formulated problem is reduced to finding the scalar function $U(r, \varphi) = H_z(r, \varphi)$, which should satisfy the inhomogeneous Helmholtz equation

$$\left[\frac{\partial^2}{\partial r^2} + \frac{1}{r} \frac{\partial}{\partial r} + \frac{1}{r^2} \frac{\partial^2}{\partial \varphi^2} + k^2 \varepsilon(r) \right] U(r, \varphi) = -\frac{4i}{r} \delta(r - r_0) \delta(\varphi), \quad (1)$$

* korip@ms.ire.rssi.ru

¹ Russia New University (RosNOU), Moscow, Russia; ² Fryazino Branch of the V. A. Kotelnikov Institute of Radio-engineering and Electronics of the Russian Academy of Sciences, Fryazino, Moscow Region, Russia. Translated from Izvestiya Vysshikh Uchebnykh Zavedenii, Radiofizika, Vol. 56, No. 5, pp. 330–336, May 2013. Original article submitted May 6, 2013; accepted May 28, 2013.

where $\delta(x)$ is a delta function, k is the wave number in free space, and the function $\varepsilon(r)$ is determined by the formula

$$\varepsilon(r) = \begin{cases} 1, & 0 < r < a; \\ \varepsilon, & a < r < b; \\ 1, & r > b. \end{cases} \quad (2)$$

At the boundaries of the layer, at $r = a$ and $r = b$, the following conditions should be fulfilled:

$$\begin{aligned} U(a-0, \varphi) &= U(a+0, \varphi), & U(b-0, \varphi) &= U(b+0, \varphi), \\ \frac{\partial U}{\partial r} \Big|_{a-0, \varphi} &= \frac{1}{\varepsilon} \frac{\partial U}{\partial r} \Big|_{a+0, \varphi}, & \frac{1}{\varepsilon} \frac{\partial U}{\partial r} \Big|_{b-0, \varphi} &= \frac{\partial U}{\partial r} \Big|_{b+0, \varphi}. \end{aligned} \quad (3)$$

The field $U(r, \varphi)$ should also satisfy the radiation conditions, i.e., at $kr \rightarrow \infty$ it should have the form

$$U(r, \varphi) = \Phi(\varphi) \sqrt{2/(\pi kr)} \exp(-ikr + i\pi/4), \quad (4)$$

where $\Phi(\varphi)$ is the radiation pattern.

The field of the diverging cylindrical wave is the solution of Eq. (1) at $\varepsilon = 1$ and is determined by the formula

$$U^0(r, \varphi) = H_0^{(2)} \left(\sqrt{r^2 + r_0^2 - 2rr_0 \cos \varphi} \right), \quad (5)$$

where $H_0^{(2)}$ is the Hankel function. The field radiation pattern $U^0(r, \varphi)$ has the form

$$\Phi^0(\varphi) = \exp(ikr_0 \cos \varphi). \quad (6)$$

3. SOLUTION METHOD

Equation (1) allows an analytical solution by the method separation of variables (Rayleigh series [2]). We present a formula for the field outside the cylinder, i.e., at $r > b$:

$$U(r, \varphi) = \frac{2i}{\pi \varepsilon k^2 ab} \sum_{m=0}^{\infty} \frac{\delta_m J_m(kr_0) H_m^{(2)}(kr) \cos(m\varphi)}{A_m(ka) D_m(kb) - B_m(ka) C_m(kb)}, \quad (7)$$

where

$$\delta_m = \begin{cases} 1, & m = 0; \\ 2, & m \geq 1, \end{cases} \quad (8)$$

$$\begin{aligned} A_m(ka) &= J'_m(ka) I_m(kna) - \frac{n}{\varepsilon} J_m(ka) I'_m(kna), \\ B_m(ka) &= J'_m(ka) K_m(kna) - \frac{n}{\varepsilon} J_m(ka) K'_m(kna), \\ C_m(kb) &= H_m^{(2)'}(kb) J_m(knb) - \frac{n}{\varepsilon} H_m^{(2)}(kb) I'_m(knb), \\ D_m(kb) &= H_m^{(2)'}(kb) K_m(knb) - \frac{n}{\varepsilon} H_m^{(2)}(kb) K'_m(knb), \end{aligned} \quad (9)$$

$$n = \sqrt{|\varepsilon|}, \quad (10)$$

J_m is the Bessel function, I_m and K_m stands for modified Bessel functions of the 1st and 2nd kind, respectively, and the prime subscript means differentiation with respect to the argument.

The radiation pattern is expressed by the formula

$$\Phi(\varphi) = \frac{2i}{\pi \varepsilon k^2 ab} \sum_{m=0}^{\infty} \frac{\delta_m J_m(kr_0) i^m \cos(m\varphi)}{A_m(ka)D_m(kb) - B_m(ka)C_m(kb)}. \quad (11)$$

Note that series (7) and (11) contain the resonance denominator

$$A_m(ka)D_m(kb) - B_m(ka)C_m(kb). \quad (12)$$

We introduce the coefficient α in accordance with the formula

$$a = \alpha b, \quad \alpha < 1. \quad (13)$$

Denominator (12) is a complex function of the parameter kb . At $kb \ll 1$ and $nkb \ll 1$, the imaginary part of Eq. (12) exceeds its real component significantly. The imaginary part of resonance denominator (12) turns to zero at the points kb_m , which are dimensionless spatial resonance frequencies. The corresponding equation for resonance frequencies is a special case of a more general equation (29) from [1], which corresponds to $\mu = 1$ and can be written as

$$\left[\frac{(kb_m)^2}{m^2 - 1} + \varepsilon + 1 \right] \left[\alpha^2 \frac{(kb_m)^2}{m^2 - 1} + \varepsilon + 1 \right] - 4\alpha^{2m} = 0, \quad m \geq 2. \quad (14)$$

Solution of quadratic equation (14) has the form

$$(kb_m)^2 = \frac{m^2 - 1}{2\alpha^2} \left[-(1 + \alpha^2)(\varepsilon + 1) \pm \sqrt{(1 - \alpha^2)^2 (\varepsilon + 1)^2 + 16\alpha^{2m+2}} \right]. \quad (15)$$

The condition of applicability of this formula is smallness of the values of $\varepsilon + 1$ and α^m .

As an example, consider the cylinder with

$$\varepsilon = -1.01, \quad \alpha = 0.3. \quad (16)$$

It is evident that in order to achieve the lowest value of the dimensionless frequency kb_m in Eq. (15), it is necessary to choose the minus sign. As a result, we obtain

$$kb_5 = 0.423. \quad (17)$$

The index $m = 5$ becomes the lowest possible one, since at $m = 4$ the right-hand part of Eq. (15) becomes negative. As the azimuthal index m increases, the resonance frequencies kb_m also increase.

Consider another case where

$$\varepsilon = -0.999, \quad \alpha = 0.3. \quad (18)$$

Then, to ensure that the right-hand part of Eq. (15) is positive, one should choose the plus sign in front of the radical in it. Specifically, we find that

$$kb_6 = 0.183. \quad (19)$$

In this case, a decrease in the index m leads to an increase in the resonance frequency kb_m .

Thus, as the index m increases, the resonance frequency can both increase and decrease. The character of this dependence is determined by the sign of the value $\varepsilon + 1$.

4. NUMERICAL RESULTS

Let us study the amplitude-frequency characteristic of the cylinder understood as the dependence of the field modulus at the point $r = b$, $\varphi = \pi$ on the dimensionless parameter kb , which is proportional to the frequency. In all calculations, the source coordinate was assumed equal to $r_0 = 0.5a$.

Figure 2 shows the amplitude-frequency characteristic of the cylinder for the two sets of problem parameters, which are determined by Eqs. (16) and (18). The calculations were performed in accordance with Eq. (7). In the presented range of dimensionless frequencies 0.1–0.9, the amplitude-frequency characteristics have several resonance peaks. The numbering of resonance frequencies is such that at the resonance frequencies kb_m the radiation pattern and the fields on the surfaces $r = a$ and $r = b$ are described by one azimuthal harmonic $\cos(m\varphi)$ with great accuracy. Note that the dimensionless values of the resonance frequencies $kb_5 = 0.42136689988$ and $kb_6 = 0.1825302075244$, which are found by rigorous numerical calculations, agree well with values (17) and (18) found by using approximate Eq. (15). Figure 2 also confirms the above-mentioned peculiarities of the functional dependence of the dimensionless resonance frequencies kb_m on the number m . Since this work considers an idealized problem, which does not allow for the thermal loss in the medium, the Q-factors of the resonances under consideration are determined only by the radiation loss. This loss turns to be rather low, which requires calculating the resonance frequency with specified high accuracy. The influence of the thermal loss on the resonance characteristics will be considered at the end of this section.

Radiation patterns at the lowest dimensionless resonance frequencies kb_5 and kb_6 are shown in Figs. 3

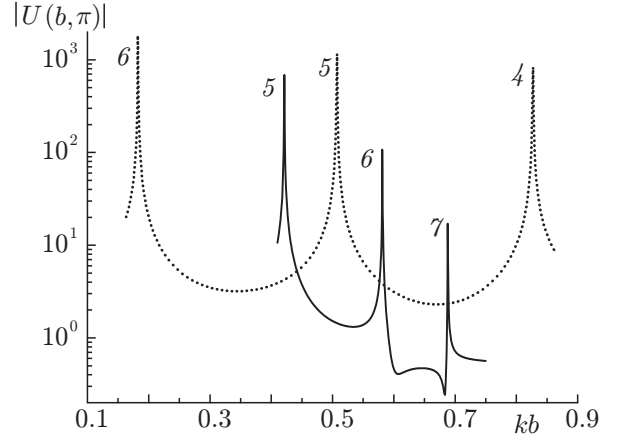


Fig. 2. Amplitude-frequency characteristics of hollow cylinders. The solid curve corresponds to $\varepsilon = -1.01$, $\alpha = 0.3$, and $r_0 = 0.5a$. The dashed curve corresponds to $\varepsilon = -0.999$, $\alpha = 0.3$, and $r_0 = 0.5a$. The numbers at the resonance peaks correspond to the azimuthal index m .

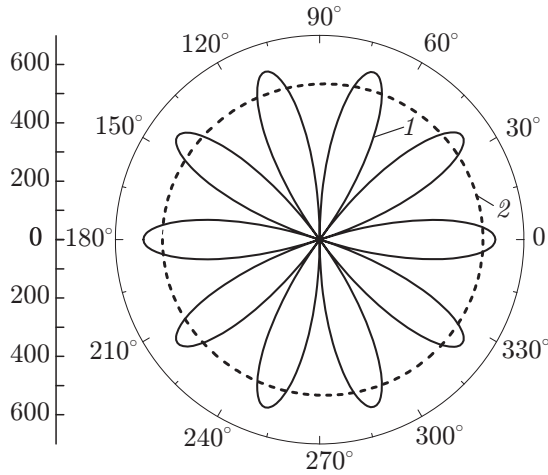


Fig. 3. Radiation pattern for the field of the hollow cylinder with $\varepsilon = -1.01$, $\alpha = 0.3$, and $r_0 = 0.5a$ at the dimensionless resonance frequency $kb_5 = 0.42136\dots$ (curve 1) and the dimensionless nonresonance frequency $kb = 0.52$ (curve 2, the scale is increased by 500 times).

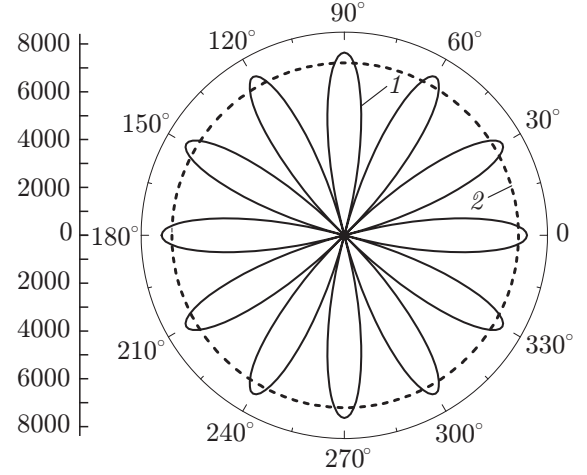


Fig. 4. Radiation pattern for the field of the hollow cylinder with $\varepsilon = -0.999$, $\alpha = 0.3$, and $r_0 = 0.5a$ at the dimensionless resonance frequency $kb_6 = 0.18253\dots$ (curve 1) and the dimensionless nonresonance frequency $kb = 0.35$ (curve 2, the scale is increased by 7000 times).

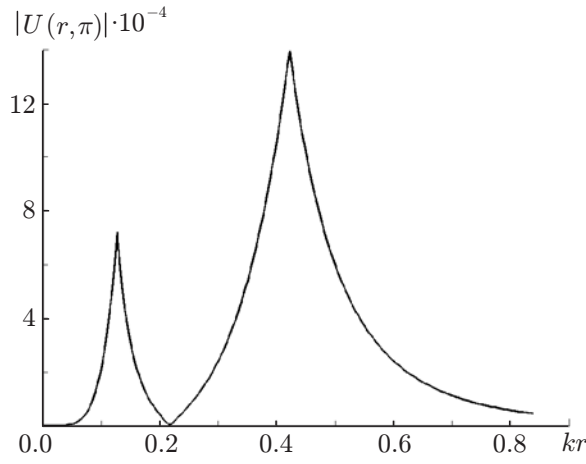


Fig. 5. Distribution of the field modulus over the radius of the hollow cylinder with $\varepsilon = -1.01$, $\nu = 10^{-5}$, $\alpha = 0.3$, and $r_0 = 0.5a$ at the dimensionless resonance frequency $kb_5 = 0.42136 \dots$

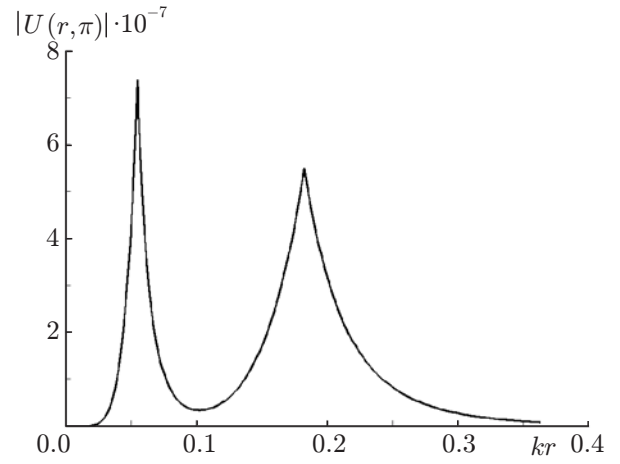


Fig. 6. Distribution of the field modulus over the radius of the hollow cylinder with $\varepsilon = -0.999$, $\nu = 10^{-8}$, $\alpha = 0.3$, and $r_0 = 0.5a$ at the dimensionless resonance frequency $kb_6 = 0.18253 \dots$

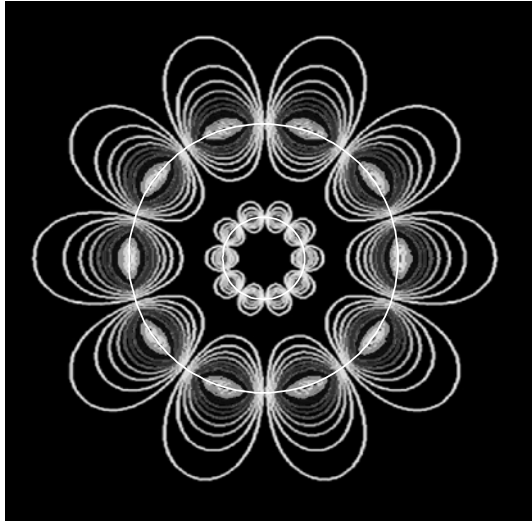


Fig. 7. Isolines of the field modulus $|U(r, \varphi)|$ in the hollow cylinder with $\varepsilon = -1.01$, $\nu = 10^{-8}$, $\alpha = 0.3$, and $r_0 = 0.5a$ at the dimensionless resonance frequency $kb_5 = 0.42136 \dots$. The circles stand for the contours of the surfaces with $r = a$ and $r = b$.

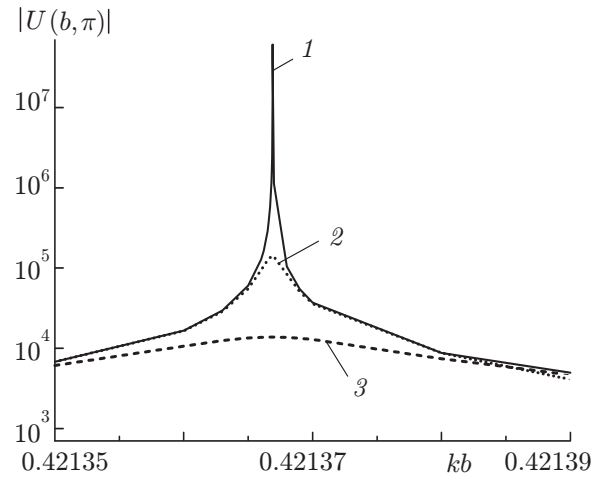


Fig. 8. Amplitude-frequency characteristics of the hollow cylinders with $\varepsilon = -1.01$, $\alpha = 0.3$, and $r_0 = 0.5a$ near the dimensionless resonance frequency $kb_5 = 0.42136 \dots$ for various dielectric losses: curves 1, 2, and 3 correspond to $\nu = 10^{-7}$, 10^{-5} , and 10^{-4} , respectively.

and 4. The patterns consist of 10 and 12 identical lobes, respectively. Figures 3 and 4 also show the radiation patterns at nonresonant frequencies. With high accuracy, they are described by the function $|\Phi(\varphi)| = 1$, which coincides with the radiation pattern of the primary field $U^0(r, \varphi)$ (see Eq. (6)). Thus, the ring-shaped layer is transparent everywhere except for the narrow resonance bands. Therefore, Figs. 3 and 4 demonstrate vividly the effect of conversion of the undirected radiation (curves 2) in the multipole radiation (curves 1) with a great number of azimuthal harmonics. Note that the amplitudes of the radiation patterns at the dimensionless resonance frequencies kb_5 and kb_6 are estimated as $6.3 \cdot 10^2$ and $7.5 \cdot 10^3$, respectively. In this case, the field distribution over the external surface of the cylinder at $r = b$ is described with graphical accuracy by the only harmonic $A_m \cos(m\varphi)$, where A_5 is of the order of 10^7 and A_6 , of 10^{11} .

The modified method of discrete sources [3, 4] was used to calculate the spatial structure of the wave

fields and study the influence of the thermal loss on the Q-factor of the resonances. The parameter $\nu = -\text{Im } \varepsilon$ was used to characterize the absorbing properties of the medium.

Figures 5 and 6 show the dependences of the fields of resonant oscillations with $kb_5 = 0.42136\dots$ and $kb_6 = 0.18253\dots$ on the radial component r . These dependences correspond to different values of the dielectric permittivity, $\varepsilon = -1.01$ and $\varepsilon = -0.999$, and differ from each other by the field behavior inside the layer. They correspond to the anti-phase and in-phase field distributions at the boundaries of $r = a$ and $r = b$ [1].

The spatial distribution of the field at the dimensionless resonance frequency $kb_5 = 0.42136\dots$ is presented in Fig. 7, which shows the isolines of the function $|U(r, \varphi)|$. The field structure consists of the surface waves, which are standing with respect to the azimuthal coordinate and localized near the cylindrical boundaries. Such waves were observed in the case of diffraction of the electromagnetic field by large bodies of a metamaterial [5, 6].

The influence of the thermal loss on the resonance properties kb_5 is illustrated in Fig. 8. An increase in the thermal loss leads to a decrease in the Q-factor of the resonance. It can be seen that even at $\nu = 10^{-5}$ the thermal loss is much higher than the radiation loss. At $\nu = 10^{-4}$, the resonance Q-factor Q is of the order of 10^4 .

5. CONCLUSIONS

Thus, a ring-shaped layer, which is made of a nonmagnetic material with dielectric permittivity close to -1 , has resonance properties in the low-frequency range. In this case, the azimuthal dependence of the fields at the resonance frequency is described by the single harmonic $\cos(m\varphi)$. The studied resonances take place only when strict requirements for the value of ε and the layer dimensions are fulfilled. Depending on the sign of the formula $\varepsilon + 1$, the resonance frequencies of the oscillations can either increase or decrease with increasing the azimuthal index m . These oscillations differ also in the character of the dependence of the field inside the layer on the radial coordinate. At the resonance frequency, the undirected radiation of the filamentary source surrounded with a ring-shaped layer is converted into multipole radiation with the radiation pattern containing $2m$ identical lobes.

This work was supported in part by the Russian Foundation for Basic Research (Project No. 12-02-00062-a).

REFERENCES

1. A. P. Anyutin, I. P. Korshunov, and A. D. Shatrov, *J. Commun. Tech. Electron.*, **58**, No. 9, 926 (2013).
2. B. Z. Katsenelenbaum, *High-frequency Electrodynamics*, Wiley-VCH, Weinheim (2006).
3. A. G. Kyurkchan, S. A. Minaev, and A. L. Solovychik, *J. Commun. Tech. Electron.*, **46**, No. 6, 615 (2001).
4. A. P. Anyutin, A. G. Kyurkchan, and S. A. Minaev, *J. Commun. Tech. Electron.*, **47**, No. 8, 864 (2002).
5. A. P. Anyutin, *J. Commun. Tech. Electron.*, **55**, No. 2, 132 (2010).
6. A. P. Anyutin, *J. Commun. Tech. Electron.*, **56**, No. 9, 1029 (2011).